Journal of Operation and Automation in Power Engineering

Vol. 8, No. 2, Aug. 2020, Pages: 172-181

http://joape.uma.ac.ir

Computationally Efficient Long Horizon Model Predictive Direct Current Control of DFIG Wind Turbines

A. Younesi, S. Tohidi [*], M. R. Feyzi

Faculty of Electrical and Computer Engineering, University of Tabriz, Tabriz, Iran.

Abstract- *Model predictive control (MPC) based methods are gaining more and more attention in power converters and electrical drives. Nevertheless, high computational burden of MPC is an obstacle for its application, especially when the prediction horizon increases extends. At the same time, increasing the prediction horizon leads to a superior response. In this paper, a long horizon MPC is proposed to control the power converter employed in the rotor side of DFIG. The main contribution of this paper is to propose a new comparative algorithm to speed up the optimization of the objective function. The proposed algorithm prevents examining all inputs in each prediction step to saving the computational time. Additionally, the proposed method along with the use of an incremental algorithm applies a sequence of weighting factors in the cost function over the prediction horizon to maximize the impact of primary samples on the optimal vector selection. Therefore, the proposed MPC strategy can predict a longer horizon with relatively low computational burden. Finally, results show that the proposed controller has the fastest dynamic response with lower overshoots compared to direct torque control and vector control method. In addition, the proposed strategy with more accurate response reduces the calculation time by up to 48% compared to classical MPC, for the prediction horizon of three.*

Keyword: *Model predictive control; computational effort; doubly fed induction generator, wind energy conversion system.*

NOMENCLATURE

P_T	Wind turbine output power
ρ	Air density
A_T	Rotor swept area
r_T	Blade radius
υ_w	Wind speed
C_P	Power coefficient of rotor blades
β	Pitch angle
λ_T	Optimal tip speed ratio (TSR)
λ_I	Intermittent TSR
r_{gb}	Gearbox ratio
n_m	Generator speed
n_T	Turbine speed
$v_{s,dq}$, $v_{r,dq}$	Stator and rotor voltage vectors
$i_{s,dq}$, $i_{r,dq}$	Stator and rotor current vectors
$\psi_{s,dq}$, $\psi_{r,dq}$	Stator and rotor flux vectors
R_s, R_r	Stator and rotor winding resistance
ω_s	Synchronous speed
ω_r	Electrical rotor speed
ω_{sl}	Slip angular speed
L_{ls}, L_{lr}	Stator and rotor leakage inductances
L_s, L_r	Stator and rotor self-inductances
L_m	Magnetizing inductance
T_e	Electromagnetic torque
P_P	Number of pole pairs
P_s, Q_s	Stator active and reactive powers
$A(t)$	State matrix in continues-time mode
B	Input matrix in continues-time mode
T_s	Control sampling time
$\Phi(k)$	State matrix in discrete-time mode
Γ	Input matrix in discrete-time mode
I	Unity matrix
k	Sample

Received: 01 Dec. 2019
Revised: 29 Mar. 2020
Accepted: 12 Apr. 2020
*Corresponding author:
E-mail: stohidi@tabrizu.ac.ir (S. Tohidi)
Digital object identifier: 10.22098/joape.2020.6703.1499
Research Paper

$v^p_{s,dq}$, $v^p_{r,dq}$	Predicted stator and rotor voltage vectors
$i^p_{s,dq}$, $i^p_{r,dq}$	Predicted stator and rotor current vectors
$v_{dc}(k)$	Measured DC link voltage
$s^p_{dr}(k)$, $s^p_{qr}(k)$	switch position combinations of RSC (*d*, *q* axis, respectively)
J	Cost function
P_d, P_q	Weighting factors

1. INTRODUCTION

Past decade has witnessed a significant breakthrough in renewable energy technologies. Among different renewable energy resources, wind power appears to be the most promising one which gets a lot of attention [1]. Due to the variable speed operation by fractionally rated back to back converter and power factor control, DFIG has been widely used for wind energy generation systems [2, 3].

Many classical control methods such as vector-based controller and field-oriented control technique have been proposed to control the DFIG [4-6]. Due to the cascade structure of proportional-integral (PI) controllers, such methods are sensitive to changes in the machine parameters and they have low dynamic response [7, 8]. However, simple structure and easy implementation made direct torque control (DTC) based methods popular in the electrical drive systems [9-11]. The main drawbacks of such controllers are the variable and high switching frequency, and high torque and current ripples [12-14]. To overcome such problems, it is proposed to use space vector modulation (SVM) alongside the DTC [15, 16]. In DTC-SVM, the switching frequency is fixed, but it requires the exact adjustment of the modulator's time. On the other hand, due to the use of PI controllers, its dynamics are lower than conventional DTC.

Direct power control with fixed switching frequency has been proposed in [17]. An adaptive control based on reinforcement learning is presented in [18]. To improve the performance of DFIG a feed-forward transient current controller is presented [19]. Fuzzy-based controllers for a DFIG connected to the wind turbine are presented in [20, 21]. The sliding mode controller is proposed to control the DFIG power [22, 23]. Similar methods are presented for AC machines in [24-26]. All such control methods have improved the performance of DFIG, but a cascade structure is still required [27, 28].

Currently, due to many benefits such as ability to control nonlinear and multivariable systems and also easy handling of real-time constraints to the objective function, methods based on predictive control are proposed for power electronics and drive systems [29-31]. Model predictive control (MPC) uses the plant model to predict the future behaviour of the system. Then, a cost function is adopted to select the most suitable switching state of the converter [32]. In [33, 34], a multiscale MPC cascade strategy is proposed to remove the gap between planning and control. A model predictive direct power control is proposed in [35], where active and reactive powers are used as the main variables in the cost function. The main problem with MPC methods is the high computational burden for online optimization of the cost function, which makes its real-time implementation complicated. To overcome this problem, several techniques are proposed in the literature.

A generalized predictive control is used to reduce the computational time in [36]. In this technique, generalized predictive control based on the finite control set model predictive control for a single-phase N-level flying capacitor multi-level rectifier used for solid-state transformers. But, in this method, adding nonlinearities and constraints to the system is very difficult. Forgoing several predictable modes is a solution that [27] has suggested to reduce the computational time of MPC. In [31], a comprehensive review has been done on seven-level topologies. A review of MPC for modular multi-level converters is presented, where some calculations are prevented by the prediction horizon of one [37]. It is worth mentioning that using the fewer number of prediction horizon results in poor selection of the control variables. Predictive direct power control with power compensation is proposed in [38, 39]. There is no need to use the PI controller and the switching table. But, the prediction horizon is still one. A predictive direct power control using power compensation is proposed in [40]. Three vector-based model predictive control has improved the dynamic response and has lowered the torque fluctuations, but it still requires an accurate calculation of voltage vector time intervals [8] has proposed. In [41], a time-efficient MPC by using binary linear programming is presented, where the switching states of the converter are taken as control inputs. A genetic algorithm is used to find superior solutions for complex problems of the MPC in [42]. In all the methods, by reducing the number of control inputs, linearization or raising the sampling frequency solutions are suggested.

In the MPC based methods, constant weighting factors are used to make trade-off between the various goals in the objective function. The prediction steps are equally weighted in the cost function. Therefore, increasing the prediction horizon results in better selection of the optimal control signal sequence, but excessive increase will make the implementation of the system impossible [43]. In this paper, a low complexity long horizon MPC strategy is proposed for DFIG in the wind energy conversion system. To reduce the computational time, in the proposed method, a comparative algorithm is used to avoid examining all the combinations of the inputs over the prediction horizon. Also, the proposed strategy applies a sequence of reduction weighting factors in the cost function to give a more accurate response with less number of the prediction horizon. The proposed approach is implemented in MATLAB/Simulink by using S-Function and is compared with the conventional MPC to evaluate its performance.

The paper is organized as follows: Section II presents the modelling of the system. The proposed MPC is explained in Section III. In Section IV, the evaluation of the proposed strategy is presented. Finally, conclusions are given in Section V.

2. SYSTEM DESCRIPTION

A. System Model

The DFIG model in the synchronous reference frame is expressed as follows[44]:

$$\mathrm{v}_{s,dq} = R_s \mathrm{i}_{s,dq} + \frac{d}{dt}\psi_{s,dq} + j\,\omega_s \psi_{s,dq} \tag{1}$$

$$\mathrm{v}_{r,dq} = R_r \mathrm{i}_{r,dq} + \frac{d}{dt}\psi_{r,dq} + j\,(\omega_s - \omega_r)\,\psi_{r,dq} \tag{2}$$

$$\psi_{s,dq} = \frac{\mathrm{v}_{s,dq} - R_s \mathrm{i}_{s,dq}}{j\,\omega_s} \tag{3}$$

$$T_e = \frac{3P_p L_m}{2\omega_s L_s}\left(-i_{qr}v_{qs} + R_s i_{qs} i_{qr} + R_s i_{ds} i_{dr} - i_{dr} v_{ds}\right) \tag{4}$$

The wind turbine output power could be calculated as

$$P_T = P_w \times C_p = \frac{1}{2}\rho A_T \upsilon_w^3 C_p \tag{5}$$

C_p represents the power coefficient of the rotor blades, which is in the range of 0.32 to 0.52 in practical wind turbines. C_p is defined below in the terms of turbine coefficients C_1 to C_7 [45].

$$C_p = C_1\left(\frac{C_2}{\lambda_I} - C_3\beta - C_4\beta^2 - C_5\right)e^{-\frac{C_6}{\lambda_I}} + C_7\lambda_T \tag{6}$$

B. Control Objectives

Since the wind speed is always changing, the DFIG output power must also be continuously adjusted to track its reference value. Generally, control goals in the DFIG are divided into two categories. The main goal is to track active and reactive power and the second goal is to limit the rotor current when the voltage drop occurs [46]. Therefore, it is suggested to use a predictive control-based method that can respond to both the problems in the best way. Also, MPC could easily handle the constraints of the system.

The DFIG stator active and reactive powers are obtained by

$$P_s = \frac{3}{2}(v_{ds} i_{ds} + v_{qs} i_{qs}) \tag{7}$$

$$Q_s = -\frac{3}{2}(v_{qs} i_{ds} - v_{ds} i_{qs}) \tag{8}$$

Then, the rotor currents are expressed in terms of stator active and reactive powers [47, 48], as:

$$i_{dr} = -\left(\frac{2L_s}{3v_{ds}Lm}\right)P_s - \left(\frac{R_s}{\omega_s L_m}\right)i_{qs} \tag{9}$$

$$i_{qr} = +\left(\frac{2L_s}{3v_{ds}Lm}\right)Q_s + \left(\frac{R_s}{\omega_s L_m}\right)i_{ds} - \left(\frac{1}{\omega_s L_m}\right)v_{ds} \tag{10}$$

3. MODEL PREDICTIVE CONTROL FOR DFIG

MPC utilizes the mathematical model of DFIG to predict the future behavior of rotor currents. Then, at each sampling period, the voltage vector which leads to the minimum objective function is selected, realizing the online optimization process. Fig. 1 shows the block diagram of the whole simulated system, which is discussed in detail in this section.

A. Discretized Model of DFIG

Calculation of predicted currents: Assuming stator and rotor current as the system states, the discrete-time model of DFIG is obtained by using Forward-Euler method as

$$\begin{bmatrix} i_{ds}^p(k+1) \\ i_{qs}^p(k+1) \\ i_{dr}^p(k+1) \\ i_{qr}^p(k+1) \end{bmatrix}_{4\times1} = \left[\Phi(k)\right]_{4\times4} \begin{bmatrix} i_{ds}(k) \\ i_{qs}(k) \\ i_{dr}(k) \\ i_{qr}(k) \end{bmatrix}_{4\times1} + \left[\Gamma\right]_{4\times4} \begin{bmatrix} v_{ds}(k) \\ v_{qs}(k) \\ v_{dr}^p(k) \\ v_{qr}^p(k) \end{bmatrix}_{4\times1} \tag{11}$$

where $i_{ds}^p(k+1)$, $i_{qs}^p(k+1)$, $i_{dr}^p(k+1)$ and $i_{qr}^p(k+1)$ are the predicted stator and rotor currents in *dq*-axes, respectively. $v_{dr}^p(k)$ and $v_{qr}^p(k)$ are the predicted rotor voltages, which are equal to

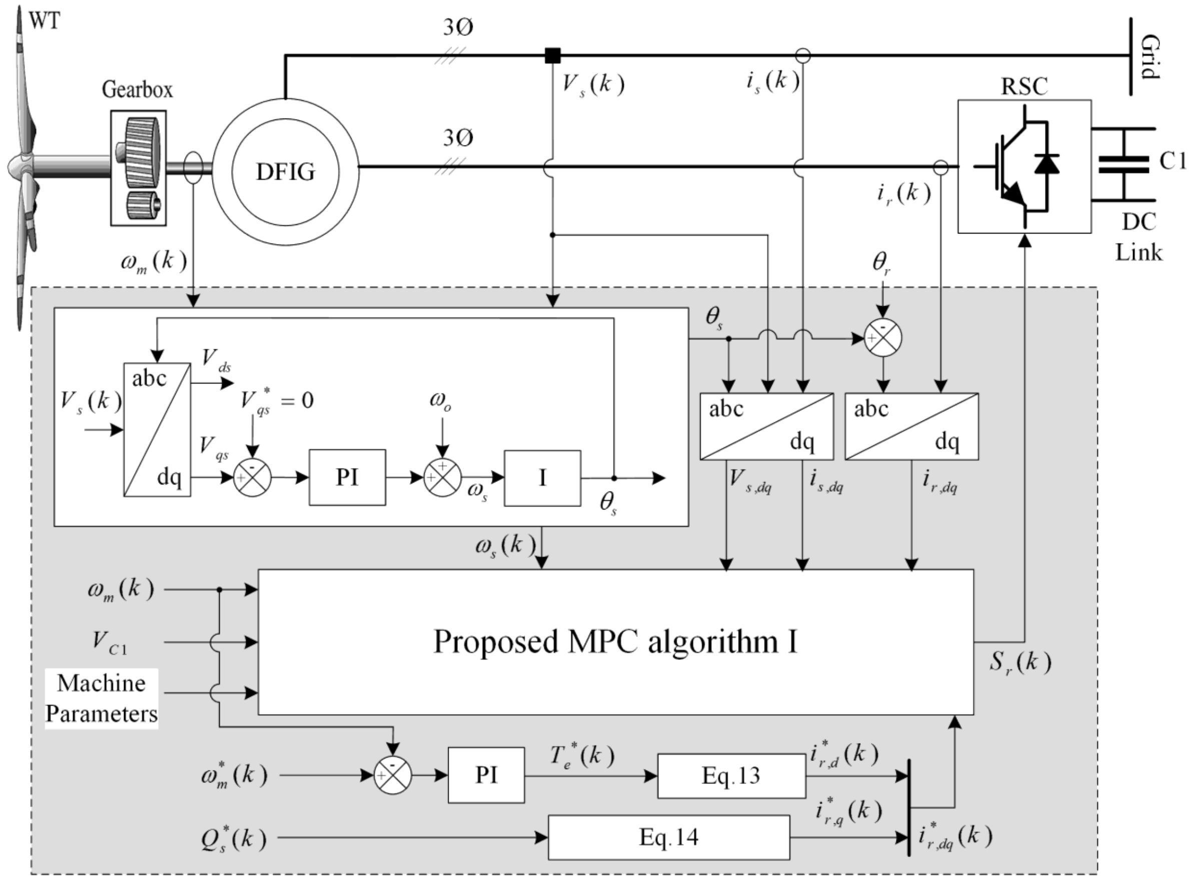

Fig.1 The DFIG-based wind power system.

$$\begin{bmatrix} v_{dr}^{p}(k) \\ v_{qr}^{p}(k) \end{bmatrix}_{2\times1} = v_{dc}(k) \begin{bmatrix} s_{dr}^{p}(k) \\ v_{qr}^{p}(k) \end{bmatrix}_{2\times1} \qquad (12)$$

Calculation of reference currents: The d-axis reference rotor current is calculated dynamically from the stator active reference P_s^* (or electromagnetic torque reference T_e^*) and, the q-axis reference rotor current is calculated from stator reactive power reference Q_s^*.

$$i_{dr}^*(k) = T_e^*(k)\left(\frac{2\omega_s L_s}{3P_p v_{ds} L_m}\right) \qquad (13)$$

$$i_{qr}^* = Q_s^*(k)\left(\frac{2L_s}{3v_{ds} L_m}\right) - \left(\frac{v_{ds}}{\omega_s L_m}\right) \qquad (14)$$

Therefore, as shown in Fig. 1, the d and q axes reference rotor current are calculated from the speed control loop and stator reactive power control loop, respectively. Finally, to compute the future value of reference rotor currents, the first-order Lagrange extrapolation is used as:

$$i_{r,dq}^*(k+1) = 2i_{r,dq}^*(k) - i_{r,dq}^*(k-1) \qquad (15)$$

B. MPC Problem Formulation

In the MPC based method, for each sample time (k) an optimal input vector sequence is obtained by optimization of a user-defined cost function. But, only the first control signal in the optimal sequence is applied to the system. According to the specified control, objectives set out in Sec. II, the cost function can be defined as:

$$J_1 = \sum_{j=1}^{N_p} P_d\left(i_{dr}^{\ *} - i_{dr}^{\ p}\right)^2 + P_q\left(i_{qr}^{\ *} - i_{qr}^{\ p}\right)^2 \qquad (16)$$

where P_d and P_q are weighting factors. They correspond to the regulation of dq reference frame rotor currents. Therefore, in this paper, P_d and P_q are set to one. According to the cost function of (16), all the prediction steps over the prediction horizon are equally weighted in the cost function. Therefore, increasing the prediction horizon results in a better selection of the optimal signal sequence, but not optimal value for the first voltage vector is obtained. To overcome this problem, the paper proposes using a variable weighting factor (Q_j) in the objective function which is decreased by increasing the prediction horizon. In other words, the proposed method along with the use of proper weight coefficients for various goals applies a sequence of weighting factors to reduce the effect of following errors over the prediction horizon. Finally, the proposed cost function can be rewritten as

$$J=\sum_{j=1}^{N_p} Q_j \begin{pmatrix} P_d\left(i_{dr}^{*}(k+j)-i_{dr}^{p}(k+j)\right)^2 \\ +P_q\left(i_{qr}^{*}(k+j)-i_{qr}^{p}(k+j)\right)^2 \end{pmatrix} \qquad (16)$$

Fig. 2, shows the flow diagram of the proposed incremental NMPC. Normally, MPC calculates the sum of objective function J over the prediction horizon N_p. The cost function can become excessively high in its initial steps for some switching states. In such cases, it is not necessary to continue the calculations for subsequent predictions. This will decrease the computational time. Thus, the use of a comparative algorithm in series with the MPC is proposed to avoid examining all the inputs in each prediction step. The algorithm I describe a step-by-step implementation of the proposed MPC.

4. SIMULATION RESULTS

In order to verify the effectiveness of the proposed MPC strategy, the model is simulated in MATLAB/Simulink to analyze the rotor voltage selection based on the proposed algorithm. The specifications of the simulated DFIG and wind turbine are given in Table I.

TABLE I
SPECIFICATIONS OF DFIG SYSTEM

DFIG Parameters	
Rated power (MW)	3
Stator line to line voltages (V)	690
Stator current (A)	2076.2
Rotor line to line voltage (V)	158.7
Rotor current (A)	2673.1
Pole pairs	2
$f_s(Hz)$	60
$R_s(m\Omega)$	1.443
$R_r(m\Omega)$	1.125
$L_{ls}(mH)$	0.094
$L_{lr}(mH)$	0.085
$L_m(mH)$	0.802
$J_m(kg.m^2)$	680
Wind Turbine Parameters	
Rated power (kW)	3000
Gain of the gear box for DFIG	96
The turbine radius (m)	43.36
Turbine constants	
$C1=0.3915,\ C2=116,\ C3=0.4,\ C4=0,$	
$C5=5,\ C6=21,\ C7=0.0192$	

* To reduce the simulation runtime, the original moment of inertia J_m is reduced to $10\ kg.m^2$.

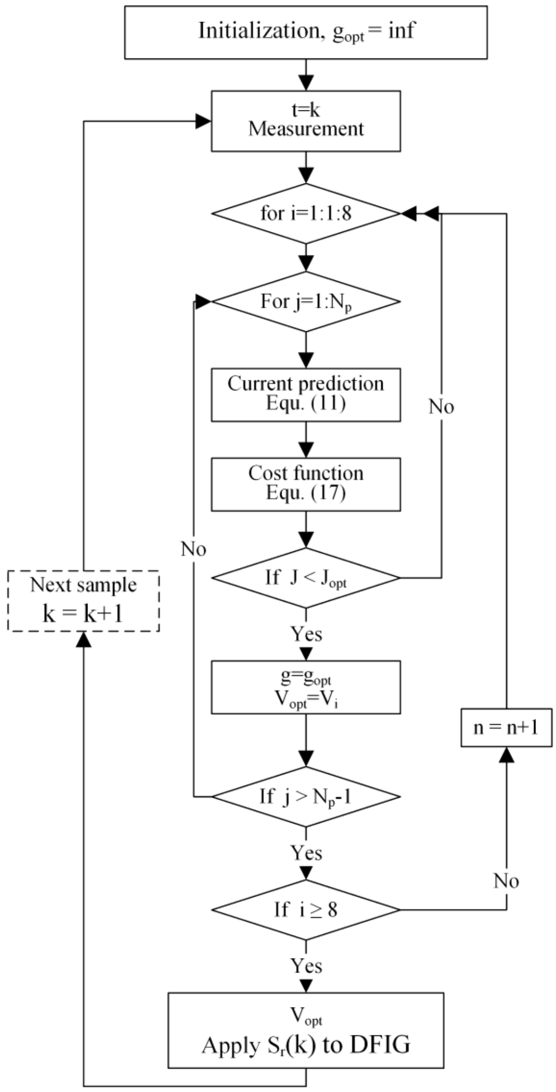

Fig. 2. Flow diagram of proposed incremental NMPC controller

A. Tracking Performance

Steady-state response of the proposed MPC, are shown in Fig. 3. The active power is kept constant at 0.75 p.u. while reactive power is zero at all times. Fig. 3 (a) clearly shows that both the voltage and current of the DFIG stator have a satisfactory. Also, Fig. 3 (b) shows generated active and reactive power equal to the specified reference values at steady state.

To evaluate the dynamic response of proposed MPC, a ramp change in wind speed is applied to increase the rotor speed from 0.75 pu (sub synchronous mode) to 1 pu (hypersynchronous mode). Fig. 4, shows the wind speed and the slip angle θ_{sl} of the DFIG.

The transient performance of the DFIG are shown in Fig. 5. In this test, reactive power is kept constant at zero, while active power varies with the variations of wind speed.

Proposed MPC algorithm I

1.	*Initialize the controller* For example: $N_p = 3$	% Initialization
2.	*Measure the* v_s, i_s, i_r *and the wind speed at the* k *moment*	% Measurements
3.	$g_{op} = \infty$	
4.	for i = 1 : 8	
5.	for j = 1 : Np	
6.	Current prediction by using (11) $i_{dr}^{p}(k+j),\ i_{qr}^{p}(k+j)$ $i_{ds}^{p}(k+j),\ i_{qs}^{p}(k+j)$	% Prediction
7.	Cost function Minimization by using (17) min $J(k)$	%Minimization of cost function
8.	$J_P^n = Q_1\left(P_d\left(i_{dr}^{*}(k+1) - i_{dr}^{p}(k+1)\right)^2 + P_q\left(i_{qr}^{*}(k+1) - i_{qr}^{p}(k+1)\right)^2\right) +$ $Q_2\left(P_d\left(i_{dr}^{*}(k+2) - i_{dr}^{p}(k+2)\right)^2 + P_q\left(i_{qr}^{*}(k+2) - i_{qr}^{p}(k+2)\right)^2\right) +$ $Q_3\left(P_d\left(i_{dr}^{*}(k+3) - i_{dr}^{p}(k+3)\right)^2 + P_q\left(i_{qr}^{*}(k+3) - i_{qr}^{p}(k+3)\right)^2\right)$	% Q_3, Q_2 and Q_1 are the weighting factor where $Q_1 \succ Q_2 \succ Q_3 \succ 0$. $Q_j = \frac{1}{2}, \frac{1}{3}, \frac{1}{4}, \ldots, \frac{1}{j+1}, \ldots, \frac{1}{N_p+1}$ $\Rightarrow Q_j = \frac{1}{j+1} \quad j = 1, 2, \ldots, N_p$
9.	if $J^i(k+j) \succ J_{opt}$ break and go to line 4	% Reference selection
10.	end if	
11.	end for	
12.	At $j = N_p$ if $J^i(k+j) \prec J_{opt}$ $J_{opt} = J^i(k+j)$	
13.	end if	
14.	end for	
15.	k = k+1 and go to line 3.	% go to the next instant (k+1) and repeat the optimization

As shown in Fig. 5, proposed nonlinear MPC (NMPC) results in superior performance of DFIG in active and reactive power tracking with faster dynamic response and lower overshoots compared to direct torque control (DTC) and vector control (VC). Fig. 6, shows the transient mode of phase a stator voltage and current and the rotor currents of the DFIG by using the proposed NMPC.

According to Fig. 6 (a) the stator is generating at unity power factor. However, the stator current amplitude increases proportionally to the rotor speed, but the stator voltage remains constant. Fig. 6 (b) shows that the amplitude of rotor currents also increases proportionally to the rotor speed, too.

B. Complexity Assessment

In this section, the influence of the proposed optimization process and a proposed comparative algorithm on the computational time is assessed. The prediction horizon is assumed to be 3 for all the cases ($N_p = 3$). The specification of different MPC strategies are listed in Table II and the output powers by using such strategies are shown in Fig. 7.

Based on Table II, each of the modifications applied to the classical MPC has a positive impact on reducing the computational burden of the system. But, the **Proposed MPC** reduces the computational time by 48%, which is of high importance for real-time implementation.

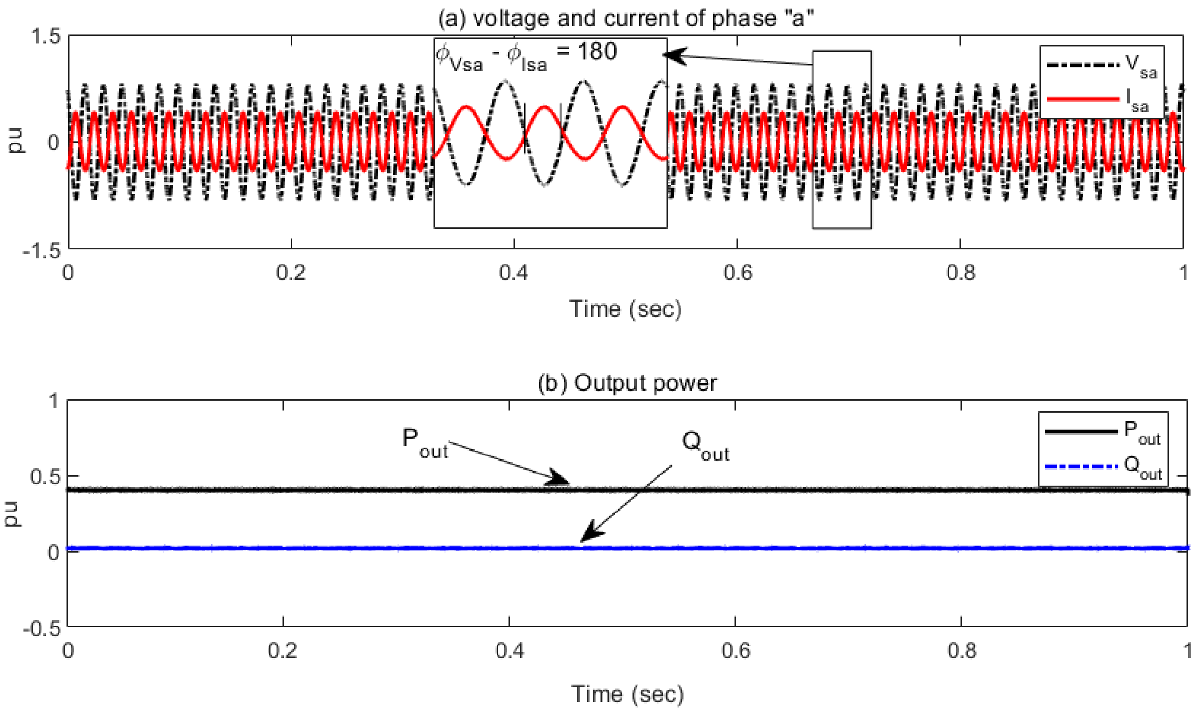

Fig. 3: Steady state performance of DFIG. (a) stator voltage and current of phase "a" and (b) Output active and reactive power.

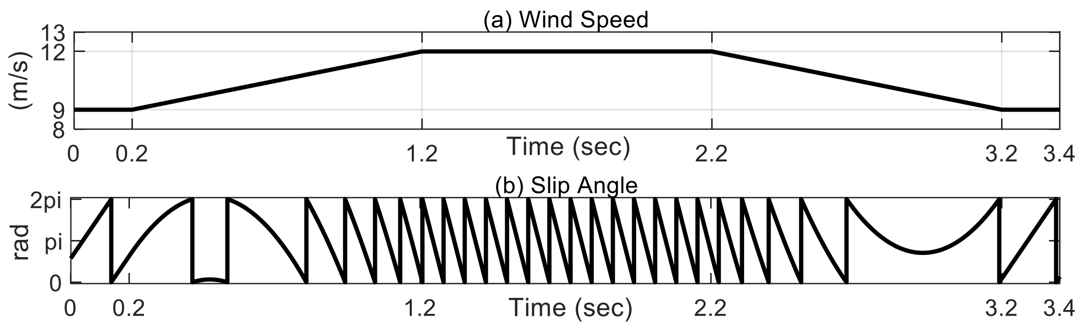

Fig. 4: wind speed and slip angle during the variation of wind speed.

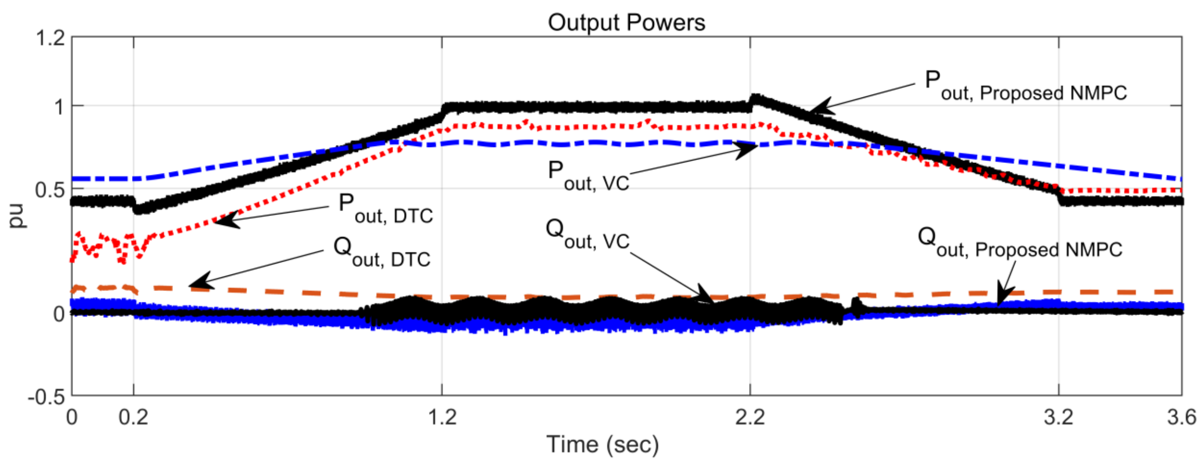

Fig. 5: Transient performance of the DFIG: Output powers (active and reactive powers).

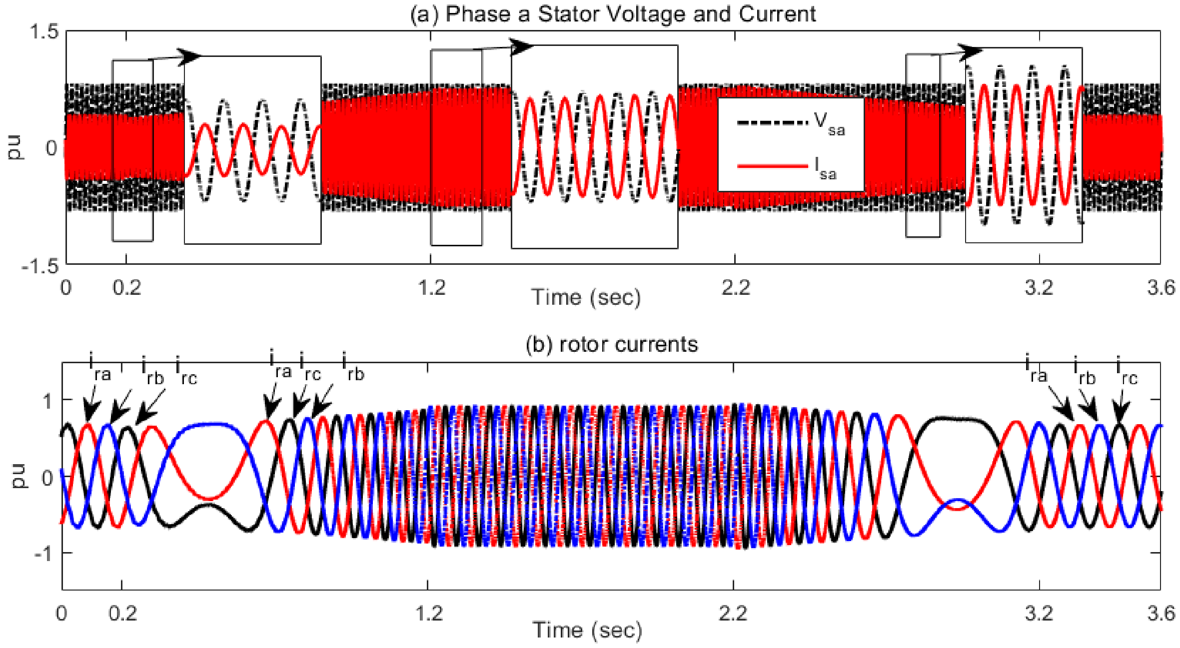

Fig. 6: Transient performance of the DFIG by using the proposed NMPC. (a) Phase-a stator voltage and current and (b) Three phase rotor currents.

TABLE II
CONTROL SPECIFICATION OF SIMULATION STEPS

Drive system	Description	Objective function	Prediction horizon (Np)	Computational time in steady state case [0-1sec], (s)	Computational time in transient [0-3.4sec], (s)
MPC-A	Classical MPC	Eq. (16), J_1	3	22.532	48.238
MPC-B	Classical MPC + Proposed optimization process	Eq. (17), J	3	19.125	36.321
MPC-C	Classical MPC + Proposed comparative algorithm	Eq. (16), J_1	3	13.786	27.955
Proposed NMPC	Classical MPC + Proposed optimization process + Proposed comparative algorithm	Eq. (17), J	3	12.805	25.119

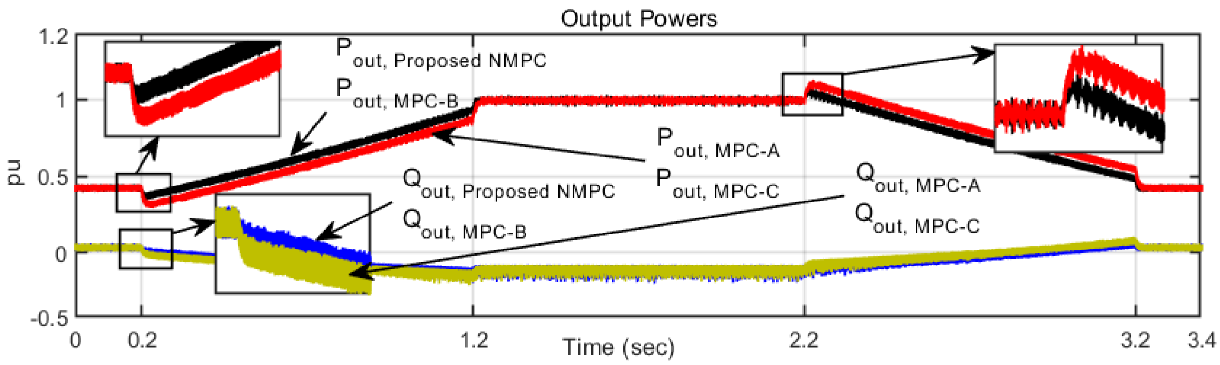

Fig. 7: The output powers of the DFIG using MPC-A, MPC-B, MPC-C and Proposed NMPC.

As shown in Fig. 7, due to the same objective function for **MPC-A** and **MPC-C**, they have the same tracking response and, for the same reason, **Proposed NMPC** and **MPC-B** have the similar responses. As observed, all the MPC strategies have a satisfactory response in active and reactive power tracking and the main difference is the computational time which is reduced by 48% in the **Proposed NMPC**.

5. CONCLUSIONS

This paper presents a computationally efficient long horizon model predictive control strategy for DFIG wind turbine systems. First, to reduce the probable errors due to the increase in the prediction horizon, a sequence of decreasing weighting factors are used over the prediction horizon. Secondly, a comparative algorithm is developed that can avoid examining all the inputs over the prediction horizon. Simulation results for a long horizon MPC show that the proposed scheme leads to satisfactory power tracking performance, and very fast running times. Compared with conventional MPC, the proposed method shows the same power tracking performance, while the computational burden has decreased by up to 48%. As a result, using the proposed strategy will make possible long horizon MPC to be implemented in practice.

REFERENCES

[1] L. L. Rodrigues, O. A. C. Vilcanqui, A. L. L. F. Murari, and A. J. S. Filho, "Predictive power control for DFIG: A FARE-based weighting matrices approach," *IEEE J. Emerging Sel. Top. Power Electron.*, vol. 7, pp. 967-975, 2019.

[2] S. Wang and L. Shang, "Fault ride through strategy of virtual-synchronous-controlled DFIG-based wind turbines under symmetrical grid faults," *IEEE Trans. Energy Convers.* pp. 1-1, 2020.

[3] A. Nafar, G. R. Arab Markadeh, A. Elahi, and R. pouraghababa, "Low voltage ride through enhancement based on improved direct power control of DFIG under unbalanced and harmonically distorted grid voltage," *J. Oper. Autom. Power Eng.*, vol. 4, pp. 16-28, 06/01 2016.

[4] R. Pena, J. C. Clare, and G. M. Asher, "Doubly fed induction generator using back-to-back PWM converters and its application to variable-speed wind-energy generation," *IEE Proc.: Electr. Power Appl.*, vol. 143, pp. 231-241, 1996.

[5] A. Tapia, G. Tapia, J. X. Ostolaza, and J. R. Saenz, "Modeling and control of a wind turbine driven doubly fed induction generator," *IEEE Trans. Energy Convers.*, vol. 18, pp. 194-204, 2003.

[6] K. K. Jaladi and K. S. Sandhu, "A new hybrid control scheme for minimizing torque and flux ripple for DFIG-based WES under random change in wind speed," *Int. Trans. Electr. Energy Syst.*, vol. 0, p. e2818.

[7] G. Abad, M. Á. Rodriguez, and J. Poza, "Two-level VSC based predictive direct torque control of the doubly fed induction machine with reduced torque and flux ripples at low constant switching frequency," *IEEE Trans. Power Electron.*, vol. 23, pp. 1050-1061, 2008.

[8] X. Wang and D. Sun, "Three-vector-based low-complexity model predictive direct power control strategy for doubly fed induction generators," *IEEE Trans. Power Electron.*, vol. 32, pp. 773-782, 2017.

[9] I. Takahashi and T. Noguchi, "A new quick-response and high-efficiency control strategy of an induction motor," *IEEE Trans. Ind. Appl.*, vol. IA-22, pp. 820-827, 1986.

[10] S. Arnalte, J. C. Burgos, and J. L. Rodríguez-Amenedo, "direct torque control of a doubly-fed induction generator for variable speed wind turbines," *Electr. Power Compon. Syst.*, vol. 30, pp. 199-216, 2002/02/01 2002.

[11] A. Izanlo, Gholamian, S.A. & Kazemi, M.V., "Using of four-switch three-phase converter in the structure DPC of DFIG under unbalanced grid voltage condition," *Electr. Eng.*, vol. 100, pp. 1925-1938, 2018.

[12] S. A. Davari, D. A. Khaburi, and R. Kennel, "An improved MPC algorithm for an induction motor with an imposed optimized weighting factor," *IEEE Trans. Power Electron.*, vol. 27, pp. 1540-1551, 2012.

[13] S. A. Davari, D. A. Khaburi, F. Wang, and R. M. Kennel, "Using full order and reduced order observers for robust sensorless predictive torque control of induction motors," *IEEE Trans. Power Electron.*, vol. 27, pp. 3424-3433, 2012.

[14] F. Niu, K. Li, and Y. Wang, "Direct torque control for permanent-magnet synchronous machines based on duty ratio modulation," *IEEE Trans. Ind. Electron.*, vol. 62, pp. 6160-6170, 2015.

[15] K. C. Wong, S. L. Ho, and K. W. E. Cheng, "Direct torque control of a doubly-fed induction generator with space vector modulation," *Electr. Power Compon. Syst.*, vol. 36, pp. 1337-1350, 2008.

[16] M. R. A. Kashkooli, S. M. Madani, and R. Sadeghi, "Improved direct torque control of DFIG with reduced torque and flux ripples at constant switching frequency," Proc. *7th Power Electron. Drive Syst. Tech. Conf. (PEDSTC)*, 2016, pp. 58-63.

[17] D. Zhi and L. Xu, "direct power control of DFIG with constant switching frequency and improved transient performance," *IEEE Trans. Energy Convers.*, vol. 22, pp. 110-118, 2007.

[18] A. Younesi, H. Shayeghi, M. Moradzadeh, "Application of reinforcement learning for generating optimal control signal to the IPFC for damping of low-frequency oscillations", *Int Trans Electr. Energy Syst.*, vol. 28, no. 2, 2018.

[19] J. Liang, W. Qiao, and R. G. Harley, "Feed-forward transient current control for low-voltage ride-through enhancement of DFIG wind turbines," *IEEE Trans. Energy Convers.*, vol. 25, pp. 836-843, 2010.

[20] H. M. Jabr, D. Lu, and N. C. Kar, "Design and implementation of neuro-fuzzy vector control for wind-driven doubly-fed induction generator," *IEEE Trans. Sustainable Energy*, vol. 2, pp. 404-413, 2011.

[21] S. A. E. M. Ardjoun, M. Denai, and M. Abid, "A robust power control strategy to enhance LVRT capability of grid-connected DFIG-based wind energy systems," *Wind Energy*, vol. 22, no. 6, 2019.

[22] X. Liu, Y. Han, and C. Wang, "Second-order sliding mode control for power optimisation of DFIG-based variable speed wind turbine," *IET Renewable Power Gener.*, vol. 11, pp. 408-418, 2017.

[23] D. Sun, X. Wang, H. Nian, and Z. Q. Zhu, "A sliding-mode direct power control strategy for DFIG under both balanced and unbalanced grid conditions using extended active power," *IEEE Trans. Power Electron.*, vol. 33, pp. 1313-1322, 2018.

[24] H. Chaoui and P. Sicard, "Adaptive fuzzy logic control of permanent magnet synchronous machines with nonlinear friction," *IEEE Trans. Ind. Electron.*, vol. 59, pp. 1123-1133, 2012.

[25] J. Yang, W. H. Chen, S. Li, L. Guo, and Y. Yan, "Disturbance/Uncertainty Estimation and Attenuation Techniques in PMSM drives; a survey," *IEEE Trans. Ind. Electron.*, vol. PP, pp. 1-1, 2016.

[26] R. Ajabi-Farshbaf, M. R. Azizian, and V. Yousefizad, "A novel algorithm for rotor speed estimation of DFIGs using machine active power based MRAS observer," *J. Oper. Autom. Power Eng.,* vol. 6, pp. 61-68, 2018.

[27] M. Preindl and S. Bolognani, "Model predictive direct speed control with finite control set of PMSM drive systems," *IEEE Trans. Power Electron.,* vol. 28, pp. 1007-1015, 2013.

[28] Y. Venkata and W. Bin, "Overview of digital control techniques," Proc. *Model Predict. Control Wind Energy Convers. Syst.*, ed: Wiley-IEEE Press, 2017, p. 512.

[29] M. Khosravi, M. Amirbande, D. A. Khaburi, M. Rivera, J. Riveros, J. Rodriguez*, et al.*, "Review of model predictive control strategies for matrix converters," *IET Power Electron.,* vol. 12, pp. 3021-3032, 2019.

[30] M. J. Khodaei, N. Candelino, A. Mehrvarz, and N. Jalili, "Physiological closed-loop control (PCLC) systems: review of a modern frontier in automation," *IEEE Access,* vol. 8, pp. 23965-24005, 2020.

[31] A. Bahrami, M. Narimani, M. Norambuena, and J. Rodriguez, "Current control of a seven-level voltage source inverter," *IEEE Trans. Power Electron.,* vol. 35, pp. 2308-2316, 2020.

[32] A. Younesi, S. Tohidi, M. R. Feyzi, and M. Baradarannia, "An improved nonlinear model predictive direct speed control of permanent magnet synchronous motors," *Int. Trans. Electr. Energy Syst.,* vol. 28, p. e2535, 2018.

[33] J. Z. Lu, "Closing the gap between planning and control: A multiscale MPC cascade approach," *Annu. Rev. Control,* vol. 40, pp. 3-13, // 2015.

[34] J. Fallah Ardashir, M. Sabahi, S. H. Hosseini, E. Babaei, and G. B. Gharehpetian, "A grid connected transformerles-s inverter and its model predictive control strategy with leakage current elimination capability," *Iran. J. Electr. Electron. Eng.,* vol. 13, pp. 161-169, 2017.

[35] C. Cheng and H. Nian, "Low-complexity model predictive stator current control of DFIG under harmonic grid voltages," *IEEE Trans. Energy Convers.,* vol. 32, pp. 1072-1080, 2017.

[36] S. Kim, R. Kim, and S. Kim, "Generalized model predictive control method for single-phase N-level flying capacitor multilevel rectifiers for solid state transformer," *IEEE Trans. Ind. Appl.,* vol. 55, pp. 7505-7514, 2019.

[37] M. Majstorović, M. E. R. Abarca, and L. Ristic, "Review of MPC techniques for MMCs," Proc. *20th Int. Symp. Power Electron.,* 2019, pp. 1-7.

[38] Y. Zhang, J. Jiao, D. Xu, D. Jiang, Z. Wang, and C. Tong, "Model predictive direct power control of doubly fed induction generators under balanced and unbalanced network conditions," *IEEE Trans. Ind. Appl.,* vol. 56, pp. 771-786, 2020.

[39] B. Hu, L. Kang, J. Cheng, Z. Zhang, J. Zhang, and X. Luo, "Double-step model predictive direct power control with delay compensation for three-level converter," *IET Power Electron.,* vol. 12, pp. 899-906, 2019.

[40] M. Moazen, R. Kazemzadeh, and M. R. Azizian, "A model-based PDPC method for control of BDFRG under unbalanced grid voltage condition using power compensa-tion strategy," *J. Oper. Autom. Power Eng.,* pp. 1-13, 2019.

[41] P. Kou, D. Liang, J. Li, L. Gao, and Q. Ze, "Finite-control-set model predictive control for DFIG wind turbines," *IEEE Trans. Autom. Sci. Eng.,* vol. 15, pp. 1004-1013, 2018.

[42] L. L. Rodrigues, A. S. Potts, O. A. C. Vilcanqui, and A. J. S. Filho, "Tuning a model predictive controller for doubly fed induction generator employing a constrained genetic algorithm," *IET Electr. Power Appl.,* vol. 13, pp. 819-826, 2019.

[43] A. Younesi, S. Tohidi, and M. R. Feyzi, "Improved optimization process for nonlinear model predictive control of PMSM," *Iran. J. of Electr. Electron. Eng.,* vol. 14, no. 3, pp. 278-288, 2018.

[44] Y. Venkata and W. Bin, "Control of DFIG wecs with voltage source converters," Proc. *Model Predict. Control Wind Energy Convers. Syst.,* ed: Wiley-IEEE Press, 2017, p. 512.

[45] Y. Venkata and W. Bin, "Chapter appendices," Proc. *Model Predict. Control Wind Energy Convers. Syst.,* ed: IEEE, 2017, p. 1.

[46] M. M. Vayeghan and S. A. Davari, "Torque ripple reduction of DFIG by a new and robust predictive torque control method," *IET Renewable Power Gener.,* vol. 11, pp. 1345-1352, 2017.

[47] X. Lie and P. Cartwright, "Direct active and reactive power control of DFIG for wind energy generation," *IEEE Trans. Energy Convers.,* vol. 21, pp. 750-758, 2006.

[48] T. Yifan and X. Longya, "A flexible active and reactive power control strategy for a variable speed constant frequency generating system," *IEEE Trans. Power Electron.,* vol. 10, pp. 472-478, 1995.